ACES Asian Chemical Editorial Society

DOI: 10.1002/asia.201601704

CHEMISTRY AN ASIAN JOURNAL Full Paper

Stimulus-responsive Nanogels | *Very Important Paper*

VIP

Stimulus-Responsive Short Peptide Nanogels for Controlled Intracellular Drug Release and for Overcoming Tumor Resistance

Linna Lyu,[a] Fang Liu,*[a] Xiaoyong Wang,[c] Ming Hu,[a] Jing Mu,[a] Haolun Cheong,[a] Gang Liu,[c] and Bengang Xing*[a, b]

Abstract: Multidrug resistance (MDR) poses a major burden to cancer treatment. As one important factor contributing to MDR, overexpression of P-glycoprotein (P-gp) results in a reduced intracellular drug accumulation. Hence, the ability to effectively block the efflux protein and to accumulate the therapeutics in cancer cells is of great significance in clinical practice. In this work, we successfully developed a smart stimulus-responsive short peptide-assembled system, termed as PD/VER nanogels, which synergistically combined the acid-activatable antitumor prodrug doxorubicin (Dox) with the P-gp inhibitor verapamil (VER) for reversing MDR. Systematic studies demonstrated that such an inhibitor-encapsulated nanogel could effectively enhance the accumulation of Dox in resistant cancer cells, thereby revealing significantly higher antitumor activity compared to free Dox molecules. This work showed that the assembly of bioactive agents with a synergistic effect into nano-drugs could provide a useful strategy to overcome cancer drug resistance.

Introduction

Currently, multidrug resistance (MDR), where cancer cells exhibit multiple resistance to numerous structure- and mechanistically independent therapeutic agents, remains a major challenge for successful cancer therapy.[1] Among the numerous mechanisms, the overexpression of the ATP-dependent drug efflux transporter P-glycoprotein (P-gp), one type of cell membrane protein that can transport a broad range of anticancer drugs out of cells, plays as an important role in reducing intracellular drug accumulation to cause serious MDR.[2]

Therefore, approaches to efficiently overcome drug resistance are highly crucial to improving the efficacy of cancer therapy. Up to now, a variety of strategies have been exploited to achieve effective reversal of MDR. Among them, the rational development of simple and unique small-molecule reagents that can suppress the efflux transporter P-glycoprotein function, thereby greatly enhancing the localized drug concentration in cancer cells, will be a promising strategy to deal with MDR.[3] So far, some small-molecule-based inhibitors have achieved promising results in early clinical trials.[4] However, lack of specificity into tumor areas and harmful effects on healthy cells may potentially impede their extensive clinical application.[5]

The latest advance of nanomedicine witnessed the great success that nanosized materials can act as promising transporters to effectively carry therapeutic agents for improving therapeutic efficacy.[6] Extensive studies have shown that these nanocarriers with appropriate particle sizes could achieve longer blood circulation and higher accumulation at the site of diseases areas (e.g., at the tumor) by taking advantages of the enhanced permeability and retention (EPR) effect.[7] Moreover, these nanomaterials may also circumvent the efflux mechanism through different internalization pathways.[8] For example, some nanoscale delivery vehicles could cross the cellular membrane based on the process of endocytosis,[9] which will prevent the encapsulated drugs from being recognized by drug efflux pumps.

Recently, nanogels, formed by the self-assembly of short peptides, have emerged as a promising material and exhibited enormous potential in the biomedical field.[10] In general, such short peptide-based nanogel materials demonstrated a unique chemical composition, mechanical properties, bioactivity, morphology, and size that could be precisely controlled to cater for various applications.[11] Furthermore, these materials also contained a higher water content and can therefore display excellent biocompatibility and higher loading capacity as com-

[a] L. Lyu, Dr. F. Liu, M. Hu, J. Mu, H. Cheong, Prof. Dr. B. Xing
Division of Chemistry and Biological Chemistry
School of Physical and Mathematical Sciences
Nanyang Technological University
Singapore 637371 (Singapore)
Fax: (+65) 6791-1961
E-mail: liuf0019@e.ntu.edu.sg
bengang@ntu.edu.sg

[b] Prof. Dr. B. Xing
Institute of Materials Research and Engineering, A*STAR
Singapore 117602 (Singapore)

[c] Dr. X. Wang, Prof. Dr. G. Liu
State Key Laboratory of Molecular Vaccinology and Molecular Diagnostics
School of Public Health
Xiamen University
Xiamen 361102 (China)

Supporting information and the ORCID identification number(s) for the author(s) of this article can be found under http://dx.doi.org/10.1002/asia.201601704.

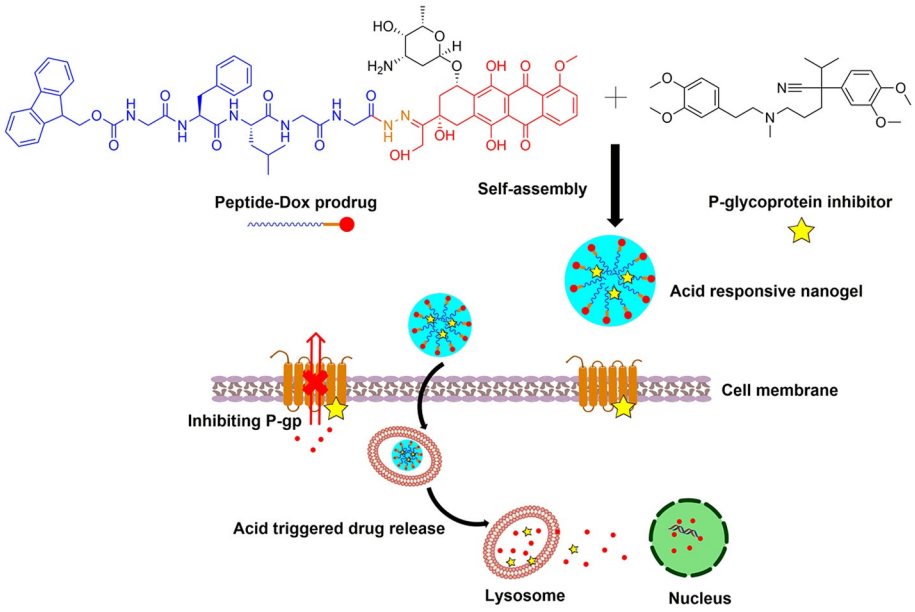

Scheme 1. Illustration of the co-assembly of peptide-Dox (PD) and P-gp inhibitor into an acid-responsive nanogel for controllable drug release to overcome cancer drug resistance.

pared to other conventional nanomaterials. Most importantly, these peptide-based nanogels can rapidly respond to various environmental stimuli, such as pH, temperature, light, enzyme or ionic strength, which thus make them attractive platforms for controllable drug release, detection of biomolecules, and regenerative medicine.[12]

Herein, we present an environmentally responsive nanogel system that can self-assemble with peptide-Dox (PD) and P-gp protein inhibitor, and can exhibit an acid-sensitive property for controlled drug release and simultaneously inhibit the efflux function of P-gp, thus effectively reversing multidrug resistance for improved tumor treatment. Typically, the chemotherapeutic agent doxorubicin (Dox) is conjugated to a short peptide sequence Fmoc-GFLGG through an acid-responsive hydrazine bond to afford a peptide-Dox prodrug (Scheme 1). This small-molecule-based peptide sequence is then co-assembled with verapamil (VER), one of the potent inhibitors for efflux protein P-gp, in aqueous solution to generate PD/VER nanogels. Upon cellular internalization, the PD/VER nanogels were accumulated in endo/lysosomes, where the acidic environment will lead to the hydrolysis of the pH-sensitive hydrazone bonds in the peptide conjugate to release free Dox drug and VER molecules. Subsequently, the released VER will suppress the efflux function of P-gp and prevent the free Dox molecules from being expelled. Therefore, the free Dox molecules will be highly accumulated in cancer cells to ensure an effective concentration, thereby countering the drug efflux effect and improving drug therapeutic efficacy.

Results and Discussion

Preparation and characterization of peptide-Dox conjugate

The designed peptide sequence Fmoc-GFLGG was prepared by standard Fmoc solid-phase peptide synthesis. A hydrazine agent was selected as a pH-sensitive moiety and introduced to the peptide sequence, which could further react with Dox molecules to afford the peptide-Dox conjugate (Figure S1 in the Supporting Information). The final products were purified by reverse-phase HPLC (Figure S2) and further characterized by NMR and mass spectrometry. After successfully obtaining the peptide-Dox conjugate, a spectroscopic analysis was carried out to investigate its photophysical properties. The absorption spectra (Figure S3a) showed that the peptide-Dox conjugate and free Dox molecules exhibited similar absorption properties from 300 to 600 nm with a maximum at 482 nm. Similarly, the fluorescence emission of the peptide-Dox conjugate showed no obvious difference from that of free Dox molecules (Figure S3b). These results indicated that the conjugation of peptide had no significant effect on the spectroscopic properties of Dox molecules.

Preparation and characterization of PD nanogels and PD/VER nanogels

We examined the possibility of the peptide-Dox conjugate to self-assemble into nanogels in water solution. To this end, a stock solution of peptide-Dox conjugate was added dropwise into pre-warmed water (60 °C, pH 7.4). The resulting solution was stirred at 60 °C for 5 min and then kept at room temperature (25 °C) for 30 min. The morphological property of the conjugate was investigated by transmission electron microscopy (TEM). The TEM images (Figure S4) revealed that the sample

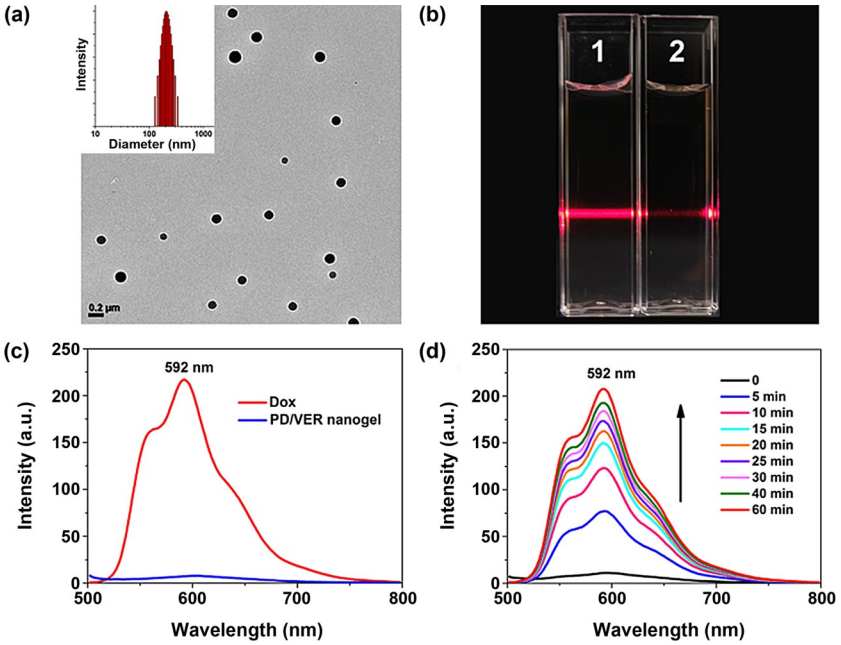

Figure 1. (a) TEM image and DLS analysis of PD/VER nanogels. (b) Tyndall effect of **1** (20 μM PD/VER nanogel in PBS buffer at pH 7.4) and **2** (20 μM PD/VER nanogel in acetate buffer at pH 5.0). (c) Fluorescence spectra of Dox and PD/VER nanogels with the same concentration (50 μM in pH 7.4 buffer) under 480 nm excitation. (d) Fluorescence enhancement of 50 μM PD/VER nanogels when dispersed in pH 5.0 buffer at different time intervals under 480 nm excitation.

prepared from peptide-Dox conjugate solution exhibited a spherical morphology, indicating the successful self-assembly of the designed peptide-Dox prodrug. Moreover, dynamic light scattering (DLS) measurements showed that the average hydrodynamic diameter of the self-assembled PD nanogels was about 198.9 ± 7.0 nm. Further studies showed that the mixture of peptide-Dox and VER in water solution also resulted in similar monodisperse spheres (PD/VER) (Figure 1 a), clearly suggesting that the addition of VER had no significant influence on the self-assembly behavior of the peptide-Dox prodrug. Furthermore, an obvious Tyndall effect, which is the scattering of light as a light beam passes through a colloid, was observed in buffer of pH 7.4 containing PD/VER (Figure 1 b), which also confirmed the successful formation of nanogels in solution.[12k,13] In addition, the DLS results shown in Figure S5 a and S5 b revealed that the critical micelle concentration (CMC) for the peptide-Dox conjugate and peptide-Dox conjugate with inhibitor (VER) is 10.0 and 9.1 μM, respectively, indicating that the peptide-Dox conjugate without and with inhibitor have similar self-assembly abilities.

We next studied the loading of Dox molecules and VER inhibitor in PD/VER nanogels by HPLC analysis. The results demonstrated an effective drug loading in the nanogel structures, and the loading amount of Dox was determined to be 44.8%, clearly suggesting the unique advantage of self-assembled nanogels to greatly increase the drug loading efficiency. In addition, HPLC measurement also indicated that the loading content of VER in PD/VER nanogels was about 3.6% (w/w), which subsequently could exert an inhibitory effect on efflux P-gp protein upon release from nanogels.

Furthermore, we performed spectroscopic studies for evaluating the self-assembling properties of nanogels. Typically, the fluorescence of PD/VER nanogels in buffer solution with different pH values was measured by using a fluorescence spectrometer. As presented in Figure 1 c, the PD/VER nanogels exhibited negligible fluorescence in pH 7.4 buffer solution. In contrast, free Dox displayed a strong fluorescence emission with the maximum excitation at 480 nm under the same conditions. Moreover, when PD/VER nanogels were dispersed in pH 5.0 buffer, the fluorescence of Dox was restored as the incubation time increased (Figure 1 d). These results implied that the fluorescence of Dox in PD/VER nanogels was quenched when the peptide-Dox conjugate assembled into nanogels, probably owing to the π–π stacking of the conjugate in nanogels.[14] Moreover, a negligible Tyndall effect was detected when the pH value of the PD/VER nanogel solution was decreased from 7.4 to 5.0 (Figure 1 b), which further indicated that the nanogels could be disassembled in an acidic environment.

Controlled drug release in buffer solution

The designed PD/VER nanogels are expected to release Dox molecules and VER inhibitors under acidic conditions (Figure 2 a). To quantitatively study the release properties of both bioactive molecules from PD/VER nanogels, HPLC analysis was carried out via detecting Dox and VER in buffer solutions at pH 7.4 and 5.0. As shown in Figure 2 c, the accumulative release percentage of VER at pH 5.0 reached to about 70.4% at 10 min. There was more release observed (up to 88.2%) after

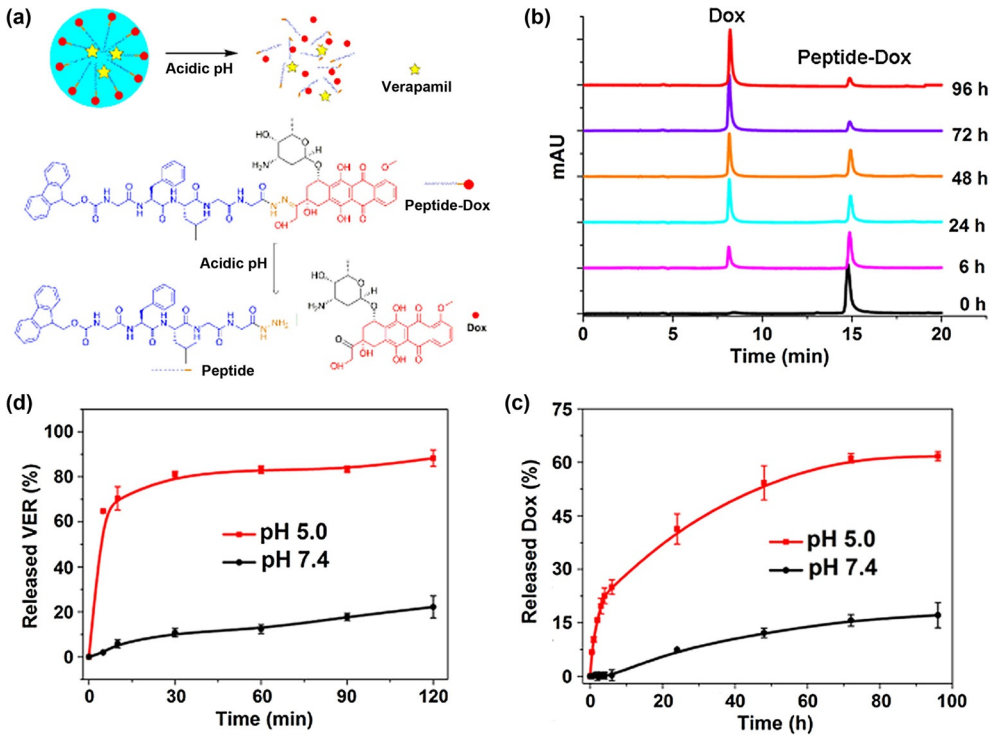

Figure 2. (a) Illustration of the acid-responsive release of VER and Dox from PD/VER nanogels. (b) HPLC traces of Dox and peptide-Dox prodrug after incubation of PD/VER nanogels at pH 5.0 and 37 °C for different times. (c) The release profiles of VER from PD/VER nanogels in PBS solution at pH 7.4 and in acetate buffer at pH 5.0 at 37 °C. (d) The cumulative release percentage of Dox from PD/VER nanogels in PBS solution at pH 7.4 and 5.0 at 37 °C.

incubation for 2 h. In comparison, only 5.8% and 22.1% of VER were released at pH 7.4 after 10 min and 2 h, respectively, indicating the rapid pH-responsive property of the designed nanogel system. As compared with VER release behavior, PD/VER nanogels exhibited a relatively slower Dox release rate. As shown in Figure 2b, a new component with a retention time of 7.5 min was observed when the PD/VER nanogel was incubated in pH 5.0 buffer solution. The new component was further confirmed to be free Dox by mass spectroscopy (Figure S6). The release amount of Dox gradually increased with prolonged incubation of the PD/VER nanogel. In addition, the cumulative release percentage of Dox in buffer solution with pH 5.0 and 7.4 were also quantitatively analyzed (Figure 2d). In the buffer solution with pH 5.0, there was 15.7% Dox release detected within 2 h, and more drug release (41.3%) was observed after 24 h incubation. Subsequently, there was 61.7% of Dox released from the nanogels within 96 h incubation in a sustained manner. As a control, a small release of Dox (up to 17.1%) was observed even after 96 h in pH 7.4 buffer. These results revealed that PD/VER nanogels were sufficiently stable at pH 7.4 and quickly disassembled at acidic conditions. Such unique environment-responsive nanogel could effectively respond to pH change and thus act as a useful therapeutic platform for controlled drug release.

Uptake and distribution of nanogels in living cells

Encouraged by the favorable pH-sensitive properties of the self-assembled nanogels, the intracellular uptake and distribution of PD/VER nanogels were further determined by monitoring the fluorescence of Dox in live cells. In this study, two cancer cell lines, that is, non-resistant A2780 cells and Dox-resistant ovarian A2780/ADR cells, were chosen as our targets mainly due to their significant difference in P-gp expression level, which have been proven by flow cytometry (Figure S7). Both A2780 cells and A2780/ADR cells were incubated with 10 μM PD/VER nanogels at 37 °C for 4 h and confocal microscopy was used for imaging analysis. As shown in Figure 3, red fluorescence signals were detected in both A2780 and A2780/ADR cells, which were mostly localized in the lysosome as confirmed by co-staining of LysoTracker green DND-26 in cell endo/lysosome organelles. The imaging results indicated that PD/VER nanogels could be internalized by both A2780 and A2780/ADR cells. Prolonged incubation (e.g., 24 h, 48 h and 72 h) of the PD/VER nanogels in A2780/ADR cells would result in the red fluorescence accumulating more in the cell nuclei than in the cytoplasm (Figure S8), demonstrating the dynamic trafficking process of the PD/VER nanogels in A2780/ADR cells. As controls, similar cellular imaging studies were also carried out with free Dox molecules. After 4 h of incubation in A2780 cells, an obvious fluorescence was observed in the cell nuclei and relatively weak fluorescence in the lysosome. In contrast, there was no significant fluorescence detected in the A2780/ADR cells. These cellular imaging studies clearly demonstrated that the designed PD/VER nanogels could work as effective platform to facilitate the delivery of anticancer drugs into resistant cancer cells, and more importantly, higher cellular internalization of therapeutic reagents could probably contribute

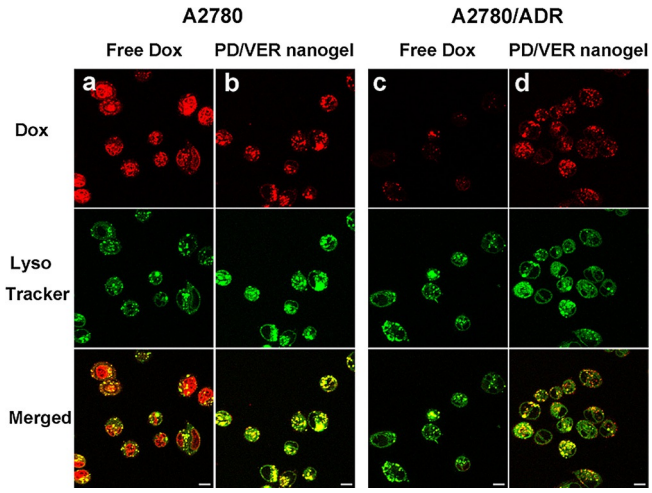

Figure 3. Confocal laser scanning microscopic images of A2780 cells and A2780/ADR cells. (a,b) A2780 cells incubated with 10 μM free Dox and10 μM PD/VER nanogel at 37 °C for 4 h, respectively; (c,d) A2780/ADR cells incubated with 10 μM free Dox and 10 μM PD/VER nanogel at 37 °C for 4 h, respectively. Green: Lyso Tracker green (λ_{Ex}: 488 nm, λ_{Em}: 500–545 nm), red: Dox (λ_{Ex}: 488 nm, λ_{Em}: 560–620 nm). Scale bar = 10 μm.

to circumventing the drug resistance and therefore dramatically improve chemotherapy efficacy.

Inhibition of VER on P-glycoprotein activity

To evaluate the possibility whether VER can act as an inhibitor to suppress P-gp efflux function, we selected the extensively used calcein AM as an indicator to study the P-gp activity. In general, calcein AM, a cell-permeable nonfluorescent dye, is cleaved by intracellular esterase to produce the impermeable fluorescent molecule calcein. Calcein AM can be actively excluded from cells expressing P-gp.[15] Therefore, the inhibition of P-gp function can increase calcein AM accumulation within the cells, which will lead to an obvious fluorescence enhancement after esterase cleavage. Here, the effect of VER on P-gp function can be assessed by measuring intracellular calcein fluorescence through flow cytometry. Typically, A2780/ADR cells were treated with VER (1 μM) for 2 h, followed by incubation with calcein AM for 20 min. As shown in Figure S9, an increased fluorescence intensity was detected in A2780/ADR cells pretreated with VER as compared to that of cells without VER pretreatment, suggesting that the activity of P-gp was greatly inhibited by VER. Moreover, flow cytometry analysis of VER-treated cells further indicated that VER had an inhibitory effect on efflux P-gp in a dose-dependent manner. Similarly, the inhibitory efficiency of VER from the PD/VER nanogel was also evaluated by calcein AM accumulation assay. As shown in Figure S10, there was no significant fluorescent change observed in A2780/ADR cells pretreated with PD nanogels, indicating that PD nanogels without VER could not enhance the accumulation of calcein in A2780/ADR cells. In contrast, pretreatment with PD/VER nanogels resulted in fluorescent enhancement, demonstrating that VER from PD/VER nanogels increased intracellular calcein concentration in A2780/ADR cells. These data showed that VER within PD/VER nanogels remarkably suppressed the P-gp efflux function in resistant cells.

With the promising inhibitory effect of VER in the PD/VER nanogel, intracellular Dox accumulation of PD/VER nanogels was further quantitatively studied using flow cytometry through measuring the fluorescence intensity of Dox. In this study, both A2780 and A2780/ADR cells were cultured and incubated with PD/VER nanogels at different time intervals. As controls, these two cell lines were also incubated with free Dox and PD nanogels, respectively. As shown in Figure 4, incubation of PD/VER nanogels with A2780 and A2780/ADR cells

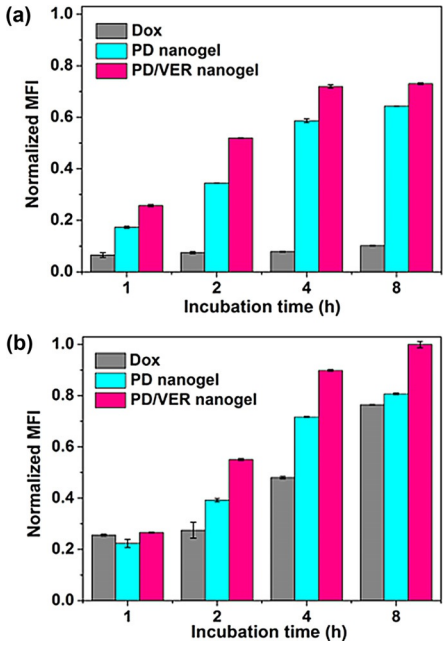

Figure 4. Quantitative analysis of mean fluorescence intensity (MFI) of Dox in (a) A2780/ADR cells and (b) A2780 cells after incubation with Dox, PD nanogels and PD/VER nanogels for various time durations (1, 2, 4, and 8 h). An equivalent Dox dosage of 10 μM was applied.

resulted in an obvious fluorescence signal in living cells. Moreover, prolonged incubation led to a significant enhancement in the fluorescence intensity due to an increased release and accumulation of Dox in cells. In addition, PD nanogels exhibited lower fluorescence intensity in both A2780 and A2780/ADR cells in comparison with PD/VER nanogel-treated cells. This observation was probably due to the inhibitory effect of VER from PD/VER nanogels on P-gp activity, which enhanced the accumulation of the released Dox molecules in cells. As comparison to incubation of PD/VER nanogels in A2780/ADR cells, cells treated with free Dox showed a greatly weaker fluorescence intensity, even after prolonged duration. These results further demonstrated that PD/VER nanogels could effectively increase the accumulation of Dox molecules in cancer cells, especially in resistant cancer cells.

Cytotoxicity

Finally, we evaluated the intracellular antitumor activity of the developed PD/VER nanogels in living cells. The cell viability was assessed by standard Tox-8 assay.[16] In this typical study, A2780 and A2780/ADR cells were incubated with PD/VER nanogels, free Dox and PD nanogels. As shown in Figure 5a and b, A2780/ADR cells incubated with 10 μM PD/VER nanogels for 48 h resulted in an obvious cytotoxicity with about 48% cell viability; a similar cell viability (43%) was also found in the sensitive A2780 cells incubated with PD/VER nanogels (10 μM). Both A2780 and A2780/ADR cells displayed an increased cytotoxicity (e.g., 16% cell viability for A2780 cells and 42% for A2780/ADR cells) when higher concentrations of PD/VER nanogels (e.g., 20 μM) were used (Figure 5a and b). Moreover, at similar effective Dox concentration, PD/VER nanogels exhibited a higher antitumor activity in A2780/ADR cells when compared with cells treated with free Dox or PD nanogels. As negative controls, similar measurements were also performed by incubation of A2780 and A2780/ADR cells with peptide (Fmoc-GFLGG-$NHNH_2$) and VER. Both peptide and VER did not lead to obvious cytotoxicity against A2780 and A2780/ADR cells, even at high concentrations (Figure 5c and d). These results strongly indicated an enhanced antitumor activity of PD/VER nanogels in resistant cancer cells. In order to quantitatively compare the cytotoxicity of free Dox and PD/VER nanogels, the IC_{50} (i.e., inhibitory concentration to produce 50% cell death)[17] values of free Dox and PD/VER nanogels were calculated in both cell lines. For A2780 cells, the IC_{50} value of free Dox was 1.9 μM, whereas a relatively higher IC_{50} value (5.5 μM) was determined for the same cell line upon incubation with PD/VER nanogels. However, unlike the potent activity observed in A2780 cells, free Dox displayed only an IC_{50} value as high as 23.3 μM in A2780/ADR cells, whereas PD/VER nanogels results in an IC_{50} of 10.2 μM, suggesting that PD/VER nanogels exhibited a higher antitumor activity than free Dox for A2780/ADR cells. Most importantly, we also investigated the resistance indices (RI, defined as the IC_{50} value of a given agent in resistant cells, divided by its IC_{50} value in sensitive cells)[18] to demonstrate the feasibility of nanogels to efficaciously overcome drug resistance. The RI value of PD/VER nanogels was determined to be 1.8 (10.2 μM/5.5 μM), which was about 6.8-fold lower than that of free Dox (12.3 = 23.3 μM/1.9 μM), suggesting that the PD/VER nanogels have the ability to effectively reverse the MDR of cancer cells. These results suggested that PD/VER nanogels offered a promising therapeutic platform to increase drug efficiency in resistant cancer cells.

Conclusions

In summary, we present a novel and smart pH-responsive cancer therapeutic platform in which chemotherapeutic and drug resistance-reversing agents were integrated for controlled drug release in resistant tumor cells. This self-assembled nanogel platform exhibited an improved cellular accumulation, controlled drug release and synergistic effect of VER and Dox. More importantly, compared to free Dox molecules alone, PD/VER nanogels had a 6.8-fold increased anti-MDR effect on Dox-resistant A2780/ADR cancer cells. This smart system provided a useful strategy to overcome cancer drug resistance for improved antitumor treatment in the near future.

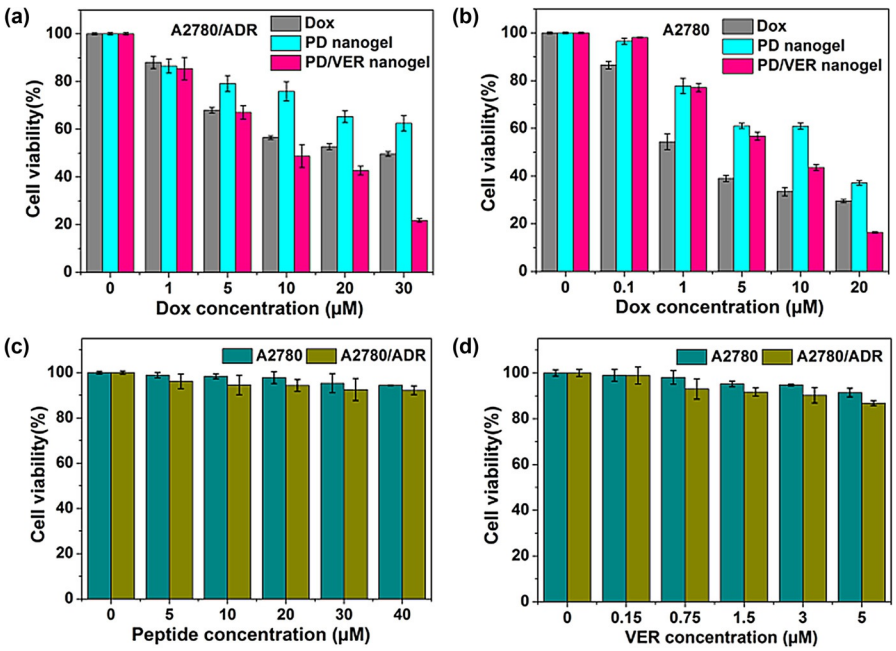

Figure 5. Cell viability assay of (a) A2780/ADR cells and (b) A2780 cells after incubation with free Dox, PD nanogels, and PD/VER nanogels for 48 h. Cell viability assay of A2780/ADR cells and A2780 cells treated with different concentrations of (c) peptide and (d) VER for 48 h.

Experimental Section

Materials

2-Chlorotrityl chloride resin and all Fmoc-amino acids were purchased from GL Biochem Ltd (Shanghai). Calcein green, AM, Lyso Tracker Green DND-26, PRMI-1640 medium and fetal bovine serum were purchased from Life Technologies. Anti-P glycoprotein antibody [UIC2] (FITC) was purchased from Abcam. All other chemicals were obtained from Sigma–Aldrich unless otherwise mentioned.

Instruments

^{1}H NMR spectra were recorded using a Bruker AV400 spectrometer (400 MHz). ESI-MS spectrometric analyses were recorded using a Thermo LCQ Deca XP Max instrument. Reverse-phase high performance liquid chromatography (HPLC) analysis was performed on a Shimadzu HPLC system with a Kromasil C-18 (250×10 mm) column at a flow rate of 3.0 mL min^{-1} for preparation and a C-18 (250×4.6 mm) column at 1.0 mL min^{-1} for analysis. Transmission electron microscopy (TEM) images were measured on an FEI EM208S transmission electron microscope (Philips) operated at 100 kV. UV/Vis absorption spectra were performed on a Cary 100 UV/Vis Spectrophotometer. Fluorescence emission spectra were recorded on a Varian Cary Eclipse Fluorescence spectrometer. The size distribution of the self-assembled nanoparticles was performed using dynamic light scattering (DLS, Brookhaven Instruments Corporation). Flow cytometry (FACS) was carried out using a Fortessa×20 instrument. Confocal laser scanning microscopy (CLSM) was performed on a LSM 510 instrument (Carl Zeiss Inc., Jena, Germany). The cell viability tests were performed using TOX-8 assay with a Tecan's Infinite M200 microplate reader.

Preparation of Peptide Fmoc-GFLGG (1)

The synthesis of peptide 1 was performed by Fmoc-based solid-phase peptide synthesis (SPPS) on a 2-chlorotrityl chloride resin. The coupling reaction of two amino acids was carried out at room temperature for 2 h using 2-(1H-benzotriazol-1-yl)-1,1,3,3-tetramethyluronium hexafluorophosphate (HBTU) and *N*,*N*-diisopropylethylamine (DIPEA) as coupling reagents. The removal of the Fmoc group was performed with 20% piperidine in dimethyformamide (DMF) for 25 min. The final peptide was cleaved from the resin by using 1% trifluoroacetic acid (TFA) and 2.5% triisopropylsilane (TIPS) in dichloromethane (DCM) for 1 min (×10). The solvent was removed via rotary evaporation, followed by precipitation of the product with cold diethyl ether. The crude product was used in the next step without further purification; Yield: 87%. MS (70 eV): *m*/*z*: 672.08 $[M+H]^+$.

Preparation of Fmoc-GFLGG-NHNH-Boc (2)

Peptide **1** (200 mg, 0.3 mmol) and *tert*-butyl carbazate (39.6 mg, 0.3 mmol) were dissolved in 5 mL DMF followed by addition of HBTU (113.7 mg, 0.3 mmol) and DIPEA (100 μL). The mixture was stirred at room temperature for 4 h and extracted twice with EtOAc. The combined organic phases were washed twice with water and thrice with saturated aqueous sodium chloride, and dried over anhydrous magnesium sulfate. After evaporation of the solvent, the residue was subjected to flash column chromatography (DCM/MeOH = 10:1) to give compound in 85% yield as a white solid. ^{1}H NMR (400 MHz, [D$_6$]DMSO, 25 °C, TMS): δ = 8.16 (d, *J* = 7.1 Hz, 1H), 8.11–7.98 (m, 2H), 7.89 (d, *J* = 7.5 Hz, 2H), 7.70 (t, *J* = 9.7 Hz, 2H), 7.52 (s, 1H), 7.42 (t, *J* = 7.4 Hz, 2H), 7.33 (t, *J* = 7.3 Hz, 2H), 7.23 (d, *J* = 4.1 Hz, 3H), 7.19–7.12 (m, 1H), 4.36–4.18 (m, 3H), 3.76 (s, 3H), 3.69–3.59 (m, 1H), 3.54 (d, *J* = 16.2 Hz, 1H), 3.42–3.34 (m, 6H), 3.04 (d, *J* = 9.0 Hz, 1H), 2.82 (dd, *J* = 25.4, 15.7 Hz, 1H), 1.49 (t, *J* = 12.1 Hz, 2H), 1.45–1.33 (m, 9H), 1.26 (dd, *J* = 10.7, 4.7 Hz, 3H), 0.86 ppm (dd, *J* = 16.5, 6.3 Hz, 6H); MS (70 eV): *m*/*z*: 808.30 $[M+Na^+]$.

Preparation of Fmoc-GFLGG-NHNH$_2$ (3)

Peptide **2** was deprotected by using 50% TFA in DCM at room temperature for 1 h. After removing the solvent, the residue was washed with cold diethyl ether to afford the product as a white solid (90%). The white solid was used for the next step without any further purification. MS (70 eV): *m*/*z*: 686.30 $[M+H]^+$.

Preparation of Fmoc-GFLGG-Dox (4)

Peptide **3** (60 mg, 0.087 mmol) and doxorubicin hydrochloride (58 mg, 0.10 mmol) were dissolved in 5 mL anhydrous methanol. The reaction was allowed to proceed in the dark at 40 °C for 24 h. The final product was purified by HPLC with elution by a linear gradient of A (50 mM ammonium acetate aqueous solution) and B (acetonitrile), monitored by UV absorbance at 280 nm and 480 nm. The linear gradient stretched over 20 minutes from *t* = 0 min at 30% solution B to *t* = 20 min at 90% solution B. The peptide-Dox conjugate was obtained after lyophilization in 46% yield as a red solid. ^{1}H NMR (400 MHz, [D$_6$]DMSO, 25 °C, TMS): δ = 11.13 (s, 1H), 10.57 (s, 1H), 8.14 (d, *J* = 8.1 Hz, 1H), 8.06 (d, *J* = 8.0 Hz, 2H), 7.98 (s, 1H), 7.95–7.83 (m, 5H), 7.67 (dd, *J* = 16.7, 6.8 Hz, 3H), 7.53 (t, *J* = 5.9 Hz, 1H), 7.39 (dd, *J* = 13.4, 6.7 Hz, 2H), 7.33–7.27 (m, 2H), 7.24–7.12 (m, 5H), 5.75 (s, 1H), 5.39 (d, *J* = 5.7 Hz, 1H), 5.31 (s, 2H), 4.98 (s, 1H), 4.54 (dd, *J* = 12.8, 8.6 Hz, 1H), 4.45 (d, *J* = 14.4 Hz, 2H), 4.33–4.17 (m, 4H), 4.15–4.08 (m, 1H), 3.96 (d, *J* = 18.8 Hz, 4H), 3.76 (d, *J* = 21.1 Hz, 2H), 3.65 (d, *J* = 6.7 Hz, 2H), 3.61 (d, *J* = 6.0 Hz, 1H), 3.51 (dd, *J* = 16.5, 5.8 Hz, 2H), 3.18 (d, *J* = 17.2 Hz, 1H), 3.02 (dd, *J* = 14.1, 4.4 Hz, 2H), 2.89 (d, *J* = 17.7 Hz, 1H), 2.78 (dd, *J* = 13.9, 9.4 Hz, 1H), 2.42–2.32 (m, 1H), 2.23 (d, *J* = 8.1 Hz, 1H), 1.93–1.79 (m, 2H), 1.69 (d, *J* = 8.2 Hz, 1H), 1.62–1.53 (m, 1H), 1.53–1.44 (m, 2H), 1.17 (d, *J* = 6.5 Hz, 3H), 0.85 ppm (dd, *J* = 16.5, 6.4 Hz, 6H); MS (70 eV): *m*/*z*: 1211.33 $[M+H]^+$.

Preparation of PD nanogels and PD/VER nanogels

Stock solutions of the peptide-Dox prodrug (50 mM, DMSO 4 μL) and of VER (50 mM, DMSO 4 μL) were co-dissolved in DMSO (2 μL) and then dropwise added to 1 mL pure water (60 °C, pH 7.4) under vigorous agitation. The resulting solution was stirred at 60 °C for 5 min and then kept at room temperature (25 °C) for 30 min. Nanogels were formed after cooling to room temperature. Free VER was removed by centrifugation at 5000 rpm for 10 min and washing with water for three times. The PD nanogels were also prepared as described for PD/VER nanogels except for the absence of VER.

Critical micelle concentration (CMC) measurements

The CMC values of peptide-Dox conjugate in the presence and absence of the inhibitor were determined by dynamic light scattering (DLS) with a laser light scattering spectrometer at 632.8 nm at room temperature (25 °C). Solutions containing different concentrations of peptide-Dox conjugates and inhibitors were tested, and the light scattering intensity was recorded for each sample.

Characterizations of PD nanogels and PD/VER nanogels

Size distributions of PD nanogels and PD/VER conjugated nanogels were measured by DLS. The morphologic examinations of PD nanogels and PD/VER nanogels were performed using TEM. In brief, 5 μL of the solution was dropped onto a carbon-coated copper grid. The excess solution was removed by using a small piece of filter paper. The sample grid was then placed to dry at room temperature prior to imaging. The encapsulated VER concentration was measured by HPLC after disruption of the PD/VER nanogels with DMSO. The disassembled PD/VER solution was injected into an HPLC column, and the concentration of VER was determined by using the absorption at 280 nm according to the standard calibration curve for pure VER.

The drug loading of the peptide-Dox prodrug is given as the Dox weight as a percentage of the total molecular weight: Drug loading (%) $= W_{Dox}/W_{total} \times 100\%$. The inhibitor VER loading capacity (DL) was calculated using the following equation: $DL = W_{VER}/W_{total} \times 100\%$, where W_{VER} is the weight of inhibitor VER and W_{total} is the total weight of nanoparticles.

Drug release in buffer solution

The release of Dox and VER from nanogels was measured in 0.1 M phosphate-buffered saline (PBS, pH 7.4) and in 0.1 M acetate buffer solution (ABS, pH 5.0) at 37 °C. Briefly, a solution of 20 μM PD/VER nanogel in either PBS or ABS was incubated at 37 °C. At different time points, 100 μL aliquots were taken out and analyzed by HPLC. The release of Dox and VER was monitored by spectroscopic analysis, in which the absorption at 480 nm was used for the detection of Dox and 280 nm for the detection of VER. The hydrolysis degree was determined based on the standard calibration curve of free Dox and VER. The drug release experiments were conducted in triplicate.

Cell culture

A2780 (Human ovarian carcinoma cells) and A2780/ADR (Adriamycin-resistant A2780 cell line) cells, obtained from European collection of cell cultures (ECACC), were cultured in RPMI 1640 medium containing 10% fetal bovine serum, 100 U mL^{-1} penicillin and 100 μg mL^{-1} streptomycin sulfate at 37 °C and 5% CO_2 in a humidified incubator. To maintain a highly drug-resistant cell population, A2780/ADR cells were periodically cultured in the presence of Dox. A2780/ADR cells were cultured in Dox-free medium for 5 days before experiments.

P-glycoprotein expression

A2780 and A2780/ADR cells were allowed to grow in 6-well plates until 80% confluence. Cells were then trypsinized and centrifuged to get a cell pellet. The cell pellet was resuspended in PBS (pH 7.4) to achieve a density of 3×10^6 cells mL^{-1}. Cells were then treated with 5 μL of FITC-labeled antibody against P-glycoprotein (UIC2). Cells were incubated for 1 h on ice according to the manufacture's protocol. After the incubation, cells were centrifuged and washed twice with ice-cold PBS and analyzed using flow cytometry (FACS) for the green fluorescence intensity. Untreated cells were taken as controls.

Calcein acetoxymethyl ester (AM) assay

A2780 or A2780/ADR cells were cultured at a density of 2×10^5 cell well^{-1} in 12-well plates for 24 h. The culture medium was then changed to fresh PRMI 1640 medium with various concentrations of VER, 10 μM PD nanogel or 10 μM PD/VER nanogel. After incubation for 2 h at 37 °C, calcein-AM was added to a final concentration of 0.5 μM, and the cells were incubated for 20 min at 37 °C. At the end of experiment, the cells were washed three times with ice-cold PBS, trypsinized and collected by centrifugation at 1200 rpm for 5 min, and finally resuspended in 300 μL of ice-cold PBS. Green fluorescence intensity was measured using a BD LSRFortessa™ ×20 FACS flow cytometer equipped with a 488 nm argon laser. Acquisition of events was stopped at 10000.

Cellular uptake

The A2780 cells or A2780/ADR cells were cultured at 2×10^5 cell dish^{-1} in a 35 mm diameter dish with a plastic bottom (ibidi GmbH, Germany) for 24 h. Serum starvation was performed in cells for 1 h, and the culture medium was changed to fresh culture medium (RPMI 1640 medium containing 10% fetal bovine serum, 100 U mL^{-1} penicillin and 100 μg mL^{-1} streptomycin sulfate) with free Dox or PD/VER nanogels (10 μM Dox and 1.5 μM VER) and then incubated at 37 °C for 3.5 h, followed by staining with Lyso Tracker Green for additional 0.5 h at 37 °C in the dark. The cells were washed three times with PBS to remove free Dox and nanogels. The cells were visualized using a Carl Zeiss LSM 510 confocal laser scanning microscope.

Flow cytometry assay

A2780 or A2780/ADR cells were seeded in 12-well plates at a density of 2×10^5 cells per well. After 24 h pre-incubation, the cells were serum starved for 1 h and then treated with Dox, PD nanogels without inhibitor, PD/VER nanogels or fresh culture medium for different time durations (i.e., 1, 2, 4 and 8 h) at an equivalent Dox concentration of 10 μM and VER concentration of 1.5 μM. At the end of experiment, the cells were washed three times with ice-cold PBS, collected by centrifugation at 1200 rpm for 5 min, and finally re-suspended in 500 μL of ice-cold PBS. The cellular fluorescence intensity of Dox was measured using flow cytometry. Each assay was repeated in triplicate.

Cell cytotoxicity

Intracellular antitumor activity measurements were performed on the basis of a standard Tox-8 assay (resazurin-based reagent, from Sigma–Aldrich). Briefly, A2780 and A2780/ADR cells were evenly seeded into 96-well plates with a density of 6.0×10^3 cells per well in 100 μL RPMI-1640 with 10% FBS and incubated at 37 °C and 5% CO_2 for 24 h. Then different concentrations of Dox, PD nanogels and PD/VER nanogels in fresh medium were added to each well. After incubation for 48 h, the medium was replaced with fresh RPMI-1640 (phenol red-free) containing 10% TOX-8 reagent, and the plate was incubated for 2 h at 37 °C. The fluorescence intensity was measured at 590 nm with excitation at 560 nm by using a Tecan's Infinite M200 microplate reader. The wells without cells but with Tox-8 reagent were set as blank controls. The cell viability was calculated as the (absorbance of treated cells)/(absorbance of untreated cells) × 100%.

Statistical analysis

Data are presented as mean ± standard error. All statistical analyses were performed using Student's *t*-test. Differences were considered statistically significant at a level of $p < 0.05$.

Acknowledgements

We gratefully acknowledge Start-Up Grant (SUG), Tier 1 (RG 64/10), (RG 11/13), (RG 35/15) awarded in Nanyang Technological University, Singapore. We also thank Kai Yang from SG Med International Pte Ltd for the helpful suggestions.

Keywords: drug delivery · glycoprotein · multidrug resistance · nanogels · peptides · self-assembly

[1] M. M. Gottesman, T. Fojo, S. E. Bates, *Nat. Rev. Cancer* **2002**, *2*, 48 – 58.
[2] G. Szakács, J. K. Paterson, J. A. Ludwig, C. Booth-Genthe, M. M. Gottesman, *Nat. Rev. Drug Discovery* **2006**, *5*, 219 – 234.
[3] a) A. H. Dantzig, D. P. de Alwis, M. Burgess, *Adv. Drug Delivery Rev.* **2003**, *55*, 133 – 150; b) M. Varma, *Pharmacol. Res.* **2003**, *48*, 347 – 359.
[4] K. N. Chi, S. K. Chia, R. Dixon, M. J. Newman, V. J. Wacher, B. Sikic, K. A. Gelmon, *Invest. New Drugs* **2005**, *23*, 311 – 315.
[5] Q. Yin, J. Shen, Z. Zhang, H. Yu, Y. Li, *Adv. Drug Delivery Rev.* **2013**, *65*, 1699 – 1715.
[6] a) M. Ferrari, *Nat. Rev. Cancer* **2005**, *5*, 161 – 171; b) J. L. Markman, A. Rekechenetskiy, E. Holler, J. Y. Ljubimova, *Adv. Drug Delivery Rev.* **2013**, *65*, 1866 – 1879; c) X. Ai, C. J. Ho, J. Aw, A. B. Attia, J. Mu, Y. Wang, X. Wang, Y. Wang, X. Liu, H. Chen, M. Gao, X. Chen, E. K. Yeow, G. Liu, M. Olivo, B. Xing, *Nat. Commun.* **2016**, *7*, 10432; d) S. E. Kim, L. Zhang, K. Ma, M. Riegman, F. Chen, I. Ingold, M. Conrad, M. Z. Turker, M. Gao, X. Jiang, S. Monette, M. Pauliah, M. Gonen, P. Zanzonico, T. Quinn, U. Wiesner, M. S. Bradbury, M. Overholtzer, *Nat. Nanotechnol.* **2016**, *11*, 977 – 985; e) C. Liang, L. Xu, G. Song, Z. Liu, *Chem. Soc. Rev.* **2016**, *45*, 6250 – 6269.
[7] C. Wang, H. Tao, L. Cheng, Z. Liu, *Biomaterials* **2011**, *32*, 6145 – 6154.
[8] S. E. Gratton, P. A. Ropp, P. D. Pohlhaus, J. C. Luft, V. J. Madden, M. E. Napier, J. M. DeSimone, *Proc. Natl. Acad. Sci. USA* **2008**, *105*, 11613 – 11618.
[9] L. M. Bareford, P. W. Swaan, *Adv. Drug Delivery Rev.* **2007**, *59*, 748 – 758.
[10] a) R. V. Ulijn, A. M. Smith, *Chem. Soc. Rev.* **2008**, *37*, 664 – 675; b) A. V. Kabanov, S. V. Vinogradov, *Angew. Chem. Int. Ed.* **2009**, *48*, 5418 – 5429; *Angew. Chem.* **2009**, *121*, 5524 – 5536; c) J. H. Collier, J. S. Rudra, J. Z. Gasiorowski, J. P. Jung, *Chem. Soc. Rev.* **2010**, *39*, 3413 – 3424; d) X. X. Zhang, H. S. Eden, X. Chen, *J. Controlled Release* **2012**, *159*, 2 – 13; e) S. Eskandari, T. Guerin, I. Toth, R. J. Stephenson, *Adv. Drug Deliv. Rev.* **2016**, DOI: 10. 1016/j.addr.2016.06.013.
[11] a) D. W. Löwik, E. H. Leunissen, M. van den Heuvel, M. B. Hansen, J. C. van Hest, *Chem. Soc. Rev.* **2010**, *39*, 3394 – 3412; b) X. M. Miao, W. Cao, W. T. Zheng, J. Y. Wang, X. L. Zhang, J. Gao, C. B. Yang, D. L. Kong, H. P. Xu, L. Wang, Z. M. Yang, *Angew. Chem. Int. Ed.* **2013**, *52*, 7781 – 7785; *Angew. Chem.* **2013**, *125*, 7935 – 7939; c) L. L. Lock, C. D. Reyes, P. Zhang, H. Cui, *J. Am. Chem. Soc.* **2016**, *138*, 3533 – 3540; d) H. Wang, Z. Feng, B. Xu, *Adv. Drug Deliv. Rev.* **2016**, DOI: 10.1016/j.addr.2016.04.008.
[12] a) G. A. Silva, C. Czeisler, K. L. Niece, E. Beniash, D. A. Harrington, J. A. Kessler, S. I. Stupp, *Science* **2004**, *303*, 1352 – 1355; b) Y. Takaoka, T. Sakamoto, S. Tsukiji, M. Narazaki, T. Matsuda, H. Tochio, M. Shirakawa, I. Hamachi, *Nat. Chem.* **2009**, *1*, 557 – 561; c) F. Zhao, M. L. Ma, B. Xu, *Chem. Soc. Rev.* **2009**, *38*, 883 – 891; d) J. Z. Du, T. M. Sun, W. J. Song, J. Wu, J. Wang, *Angew. Chem. Int. Ed.* **2010**, *49*, 3621 – 3626; *Angew. Chem.* **2010**, *122*, 3703 – 3708; e) Y. Gao, J. F. Shi, D. Yuan, B. Xu, *Nat. Commun.* **2012**, *3*, 1033; f) H. M. Wang, J. Wei, C. B. Yang, H. Y. Zhao, D. X. Li, Z. N. Yin, Z. M. Yang, *Biomaterials* **2012**, *33*, 5848 – 5853; g) A. G. Cheetham, P. Zhang, Y. A. Lin, L. L. Lock, H. Cui, *J. Am. Chem. Soc.* **2013**, *135*, 2907 – 2910; h) C. H. Ren, H. M. Wang, D. Mao, X. L. Zhang, Q. Q. Fengzhao, Y. Shi, D. Ding, D. L. Kong, L. Wang, Z. M. Yang, *Angew. Chem. Int. Ed.* **2015**, *54*, 4823 – 4827; *Angew. Chem.* **2015**, *127*, 4905 – 4909; i) Y. Yuan, L. Wang, W. Du, Z. L. Ding, J. Zhang, T. Han, L. N. An, H. F. Zhang, G. L. Liang, *Angew. Chem. Int. Ed.* **2015**, *54*, 9700 – 9704; *Angew. Chem.* **2015**, *127*, 9836 – 9840; j) H. Zhang, J. Fei, X. Yan, A. Wang, J. Li, *Adv. Funct. Mater.* **2015**, *25*, 1193 – 1204; k) Y. Zhao, F. Chen, Y. Pan, Z. Li, X. Xue, C. I. Okeke, Y. Wang, C. Li, L. Peng, P. C. Wang, X. Ma, X. J. Liang, *ACS Appl. Mater. Interfaces* **2015**, *7*, 19295 – 19305.
[13] J. Ping, Y. Wang, Q. Lu, B. Chen, J. Chen, Y. Huang, Q. Ma, C. Tan, J. Yang, X. Cao, Z. Wang, J. Wu, Y. Ying, H. Zhang, *Adv. Mater.* **2016**, *28*, 7640 – 7645.
[14] a) Z. Chen, A. Lohr, C. R. Saha-Moller, F. Wurthner, *Chem. Soc. Rev.* **2009**, *38*, 564 – 584; b) F. Biedermann, E. Elmalem, I. Ghosh, W. M. Nau, O. A. Scherman, *Angew. Chem. Int. Ed.* **2012**, *51*, 7739 – 7743; *Angew. Chem.* **2012**, *124*, 7859 – 7863.
[15] J. A. Ludwig, G. Szakacs, S. E. Martin, B. F. Chu, C. Cardarelli, Z. E. Sauna, N. J. Caplen, H. M. Fales, S. V. Ambudkar, J. N. Weinstein, M. M. Gottesman, *Cancer Res.* **2006**, *66*, 4808 – 4815.
[16] D. Liu, *Bull. Environ. Contam. Toxicol.* **1981**, *26*, 145 – 149.
[17] Z. R. Peng, W. H. Zhong, J. Liu, P. T. Xiao, *Undersea Hyperbaric Med.* **2010**, *37*, 141 – 150.
[18] S. Kunjachan, A. Blauz, D. Mockel, B. Theek, F. Kiessling, T. Etrych, K. Ulbrich, L. van Bloois, G. Storm, G. Bartosz, B. Rychlik, T. Lammers, *Eur. J. Pharm. Sci.* **2012**, *45*, 421 – 428.

Manuscript received: December 16, 2016
Accepted Article published: January 9, 2017
Final Article published: February 2, 2017